Jpn J Ophthalmol
DOI 10.1007/s10384-014-0319-3

THE OFFICIAL INTERNATIONAL JOURNAL OF THE JAPANESE OPHTHALMOLOGICAL SOCIETY

LABORATORY INVESTIGATION

Evaluation of electrochemically treated bulk electrodes for a retinal prosthesis by examination of retinal intrinsic signals in cats

Hiroyuki Kanda · Toshifumi Mihashi · Tomomitsu Miyoshi · Yoko Hirohara · Takeshi Morimoto · Yasuo Terasawa · Takashi Fujikado

Received: 10 October 2013 / Accepted: 14 February 2014

Abstract
Purpose Our goal was to determine the feasibility of using electrochemically treated bulk platinum electrodes with large charge injection capacity for a retinal prosthesis.
Methods Seven eyes of seven cats were studied. Small retinal areas were focally stimulated with electrochemically treated bulk electrodes ($\varphi = 500$ μm) placed in a scleral pocket. Fundus images with near-infrared (800–880 nm) light were recorded, and a 2D map of the reflectance changes elicited by the electrical currents was constructed by subtracting the images taken before stimulation from those taken after stimulation. The impedance of each electrode was measured at 1 kHz. The degree of retinal elevation by the electrode was measured by optical coherence tomography. Scleral thickness where the electrode array was inserted was measured in histologic sections.
Results The diameter of reflectance changes (full width at half maximum) was 0.42 ± 0.22 mm [mean ± standard deviation (SD)] in minor axes and 1.46 ± 0.82 mm in major axes. The threshold current decreased with a reduction in the residual scleral thickness ($R^2 = 0.9215$; $P = 0.0002$); it also decreased with an increase in retinal elevation ($R^2 = 0.6259$; $P = 0.0111$).The threshold current also decreased with an increase in electrode impedance ($R^2 = 0.2554$; $P = 0.0147$).
Conclusions Electrochemically treated porous platinum electrodes can stimulate localized retinal areas. The threshold current necessary to stimulate the retina was influenced by residual scleral thickness and the electrode tightness of fit against the sclera.

Keywords Optical imaging · Intrinsic signal · Porous electrodes · Electrical stimulation · Retinal prosthesis

H. Kanda · T. Morimoto · T. Fujikado (✉)
Department of Applied Visual Science, Osaka University Graduate School of Medicine, 2-2 Yamadaoka, Suita, Osaka 565-0871, Japan
e-mail: fujikado@ophthal.med.osaka-u.ac.jp

T. Mihashi
Department of Innovative Research Initiatives, Tokyo Institute of Technology, Yokohama, Japan

T. Miyoshi
Department of Integrative Physiology, Osaka University Graduate School of Medicine, Osaka, Japan

Y. Hirohara
Optical Engineering Laboratory, Topcon Corporation, Tokyo, Japan

Y. Terasawa
Vision Institute, NIDEK Company, Gamagori, Japan

Introduction

Retinitis pigmentosa (RP) is one of the leading causes of blindness and is characterized by degeneration of photoreceptors. At the advanced stage, RP patients have little or no functional vision, and no effective treatment exists for this disease. To restore some vision to these patients, the strategy of stimulating residual retinal neurons using a retinal prosthesis has been extensively studied [1–10]. A retinal prosthesis is a medical device that has the potential of restoring vision by stimulating the retina with electrical pulses. Retinal prostheses are classified into three types: subretinal [1–3], epiretinal [4, 5], and suprachoroidal–transretinal stimulation (STS) [6–11]. In the epiretinal and subretinal types, the implanted stimulating electrode is attached directly to the retina, so the

Published online: 01 May 2014

possibility of retinal damage by surgery cannot be excluded [2, 5]. On the other hand, the STS prosthesis is inserted into a scleral pocket [8] or suprachoroidal space [7, 9], and the electrodes are not in direct contact with the retina, so only minimal surgical damage to the retina can occur [6, 11].

When using our STS-type retinal prosthesis, current pulses of up to 0.5 μC/phase must be delivered safely [11]. This exceeds the charge delivery capacity of conventional planar platinum electrodes [12]. To obtain a 0.5-μC/phase charge injection, we previously proposed a 0.5-mm-high bullet-shaped electrode using bulk micromachining [13]. However, in a few cases of chronic implantation in rabbits, retinal damage due to mechanical pressure from the electrode was observed (data not shown). To decrease mechanical pressure to the retina by lowering the electrode height, we developed a technique for increasing the surface area through electrochemical etching [14]. Increasing the surface area enabled a 40 % reduction in electrode height because of the high charge injection capacity. This new electrode was 0.3 mm in height [14]. However, the electrochemically treated electrode has not been evaluated for its effectiveness in stimulating retinal neurons.

The effects of using multiple electrodes for stimulating the retina have been evaluated in vitro using microfabricated multielectrode arrays [15] or by electrophysiologic methods on the visual cortex [16, 17]. However, it had been difficult to evaluate the resolving power of the retinal prosthesis in situ. We showed that functional imaging of the intrinsic retinal signal can be effective for evaluating the area stimulated by an STS prosthesis [18]. In that study, we used a single platinum electrode attached to the sclera.

The purpose of the study reported here was to evaluate electrochemically treated multiple platinum electrodes in stimulating the retina when implanted in a scleral pocket. We used retinal functional imaging not only to determine whether the retina was activated but also to determine the effect of STS array placement in the sclera pocket on the activation threshold.

Materials and methods

Cats

Seven eyes of seven cats (both sexes; weight 3–4 kg) were used for these experiments. All experiments were performed in accordance with the Association for Research in Vision and Ophthalmology (ARVO) Statement for the Use of Animals in Ophthalmic and Visual Research, and the procedures were approved by the Animal Research Committee of the Osaka University Medical School.

General preparation

The cats were initially given an intramuscular injection of ketamine hydrochloride (25 mg/kg) and an intraperitoneal injection of atropine sulfate (0.1 mg/kg). Each animal was anesthetized with an intravenous infusion of pentobarbital sodium (1 mg/kg/h) and paralyzed with pancuronium bromide (0.2 mg/kg/h) mixed with Ringer's solution and glucose (0.1 g/kg/h). Each cat was artificially ventilated with a mixture of nitrous oxide/oxygen (N_2O/O_2) (1:1); end-tidal carbon dioxide (CO_2) concentration was controlled at 4.0–5.5 % by altering ventilation frequency and volume. In addition to continuous monitoring of the expired CO_2, intratracheal pressure and electrocardiogram were also monitored. The body temperature was maintained with a heating pad at 38 °C. The pupils were dilated with 1 % atropine sulfate (Nihon Tenganyaku Institute, Nagoya, Japan) and 5 % phenylephrine hydrochloride (Kowa Company, Nagoya, Japan).

Optical imaging of the retina

The ocular fundus was monitored using a fundus camera (TRC-50LX; Topcon Corporation, Tokyo, Japan) with a digital CCD camera (C8484; Hamamatsu Photonics, Hamamatsu, Japan). The camera has a resolution of 1,280 × 1,024 pixels; however, the binning mode was used to obtain maximum light sensitivity, and the resolution was reduced to 320 × 256 pixels. To evaluate reflectance, a 12-bit digitizer was used, and a grayscale value (GSV) of 4,096 was obtained for each pixel. A halogen lamp was used to illuminate the posterior fundus, and a band-pass filter was inserted in the optical path to limit the wavelength passing to the fundus to between 800 and 880 nm. All experiments were performed in a dark room after 30 min of dark adaptation.

During each experiment, gray-scale images of the fundus were continually recorded at intervals of 25 ms for 25 s between 2 s before and 20 s after electrical stimulation. Trials were repeated ten times in each session. To improve the signal-to-noise ratio (SNR), images in all trials were averaged for each time point from the onset of the electrical stimulation. In addition, ten serial images were averaged every 250 ms. A 2D map of reflectance changes was obtained by subtracting raw fundus images taken before from those taken after stimulation.

Electrophysiologic recording from the optic chiasm

To record responses of retinal ganglion cells elicited by the electrical stimulation, bipolar stainless-steel electrodes were stereotaxically placed in the optic chiasm. The electrode was inserted from the cortical surface 13–14 mm

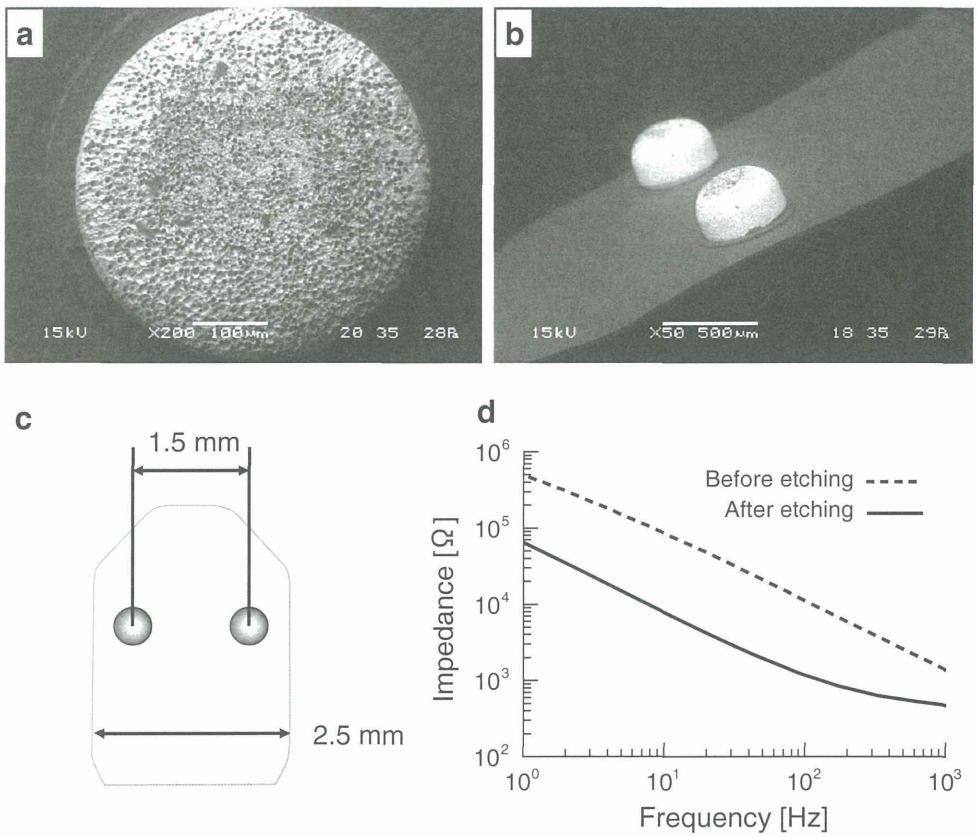

Fig. 1 Electrochemical treatment to platinum bulk electrode. **a** Scanning electron microscopic (SEM) image of the pitted electrode. A high density of pits can be seen on the surface of the bullet-shaped electrode, which increased the surface area. The pores were made by electrochemical etching. **b** SEM image of the stimulating electrode array. **c** SEM array consists of two porous electrodes with a center-to-center distance of 1.5 mm. **d** Frequency dependence of electrode impedance. The *dashed line* indicates impedance of the electrode before etching. The *solid line* indicates impedance of the electrode after etching

anterior to the ear bar and 1–2 mm ipsilateral to the midline. The depth of the electrode tip was 23–26 mm from the cortical surface. The flash-evoked response from the electrode was monitored to determine whether the electrode was in the optic chiasm. The recorded signal from the bipolar electrode was amplified 5,000 times and band-pass filtered from 10 Hz to 5 kHz using an AC-amplifier (Model 1800 Microelectrode AC amplifier; A-M SYSTEMS, Sequim, WA, USA) and a signal conditioner (LPF-202A; Warner Instruments, Hamden, CT, USA). The amplified signal was recorded with a signal processor (Power 1401; Cambridge Electronic Design, Cambridge, UK) with a sampling frequency of 50 kHz and analyzed offline with Signal 4 software (Cambridge Electronic Design). The signal was also monitored on an oscilloscope and an audio monitor in real time.

Creation of a porous electrode

The electrode array consisted of electrochemically treated platinum bulk electrodes. Each electrode was bullet shaped and created by a lathe from a bulk 0.5-mm-diameter platinum bar [14]. Electrochemical etching was done to create a porous surface that would allow for a high charge injection capacity. Electrochemical etching was done by applying a +5-volt DC to the electrode for 1 s, followed by −5-volt DC for another 1 s. The entire process was performed with the electrode immersed in phosphate-buffered saline (PBS) [14]. This voltage cycle was repeated for 15.5 h at room temperature. Each electrode was 0.5 mm in diameter and 0.3 mm in height (Fig. 1a, b).

Before stimulating the retina with the porous electrode, the effects of the porous surface treatment were evaluated by measuring the impedance and performing a spectroscopic analysis of porous and nonporous electrodes. These measurements were performed with the electrodes immersed in PBS at room temperature. The surface geometry of the electrodes was examined with a scanning electron microscope (SEM). We measured electrode charge injection capacity, which is defined as the maximum charge density capacity without deviation of the platinum water window [−0.6 to +0.8 V vs. silver/silver chloride (Ag/AgCl)] during the charge injection. Current pulses consisted of 500-µs duration and cathodic-first pulses at 30 Hz for measurements. We created an electrode array to deliver electrical stimulation to the retina. Each array comprised two porous electrodes with a center-to-center distance of 1.5 mm (Fig. 1c). The basal plate of the electrode array was made of paryline.

Electrical stimulation of the retina

To implant the electrode array, a horizontal skin incision was made about 20 mm from the lateral canthus. The temporal orbital bone was removed to expose the sclera, and the lateral rectus muscle and retractor oculi muscle were cut. A scleral pocket incision of approximately 5 × 5 mm was made with a crescent knife in the superotemporal area 15 mm from the corneal limbus and just above the long posterior ciliary artery. The electrode array was inserted into the scleral pocket. The lead wire was sutured to the scleral surface. A silver plate (5 × 10 mm) was placed under the scalp as the return electrode. After electrode array implantation, optical coherence tomography (OCT) images of the posterior pole of the eye in the implantation area were obtained with iVue (Optovue, Fremont, CA, USA). This OCT device captures cross-sectional images of the retina and choroid. We evaluated the height of the lump created by the electrode (Fig. 7c). OCT examinations were performed on cat nos. 3, 4, 5, 6, and 7. Impedance between the stimulating and return electrode was measured at 1 kHz using an LCR meter (chemical impedance meter 3532-80; HIOKI, Ueda Japan) on all cats. Impedances were measured just before and 1, 4, and 17 h after onset of the stimulation trial. For each trial, 4-s pulse trains were delivered to the retina. The pulse trains consisted of cathodic-first biphasic pulses with a frequency of 20 Hz, and pulse duration/phase was 0.5 ms. Cathodic-first biphasic pulses were used in part because their charge injection capacity is higher than that of anodic-first biphasic pulses [13]. To determine the correlation between the stimulus current and the area of reflectance changes, the electrical current was systematically increased from 0.03 to 2.0 mA. All stimulating pulses were generated using an STG4008 stimulator (Multi Channel Systems MCS, Reutlingen, Germany). The mass-evoked potential at the optic chiasm stimulated by STS was monitored on an oscilloscope to confirm the effectiveness of the electrical stimulation.

Histologic analyses

Histologic studies were performed on cat nos. 4, 5, 6, and 7 to evaluate scleral thickness where the electrode array was inserted. After the experiments, the electrode array was removed from the eye, and the cat was deeply anesthetized with pentobarbital sodium (somnopentyl; Kyoritsu Seiyaku, Tokyo, Japan). The eye was enucleated and fixed in 2 % paraformaldehyde and 1.25 % glutaraldehyde in PBS. The eye was embedded in paraffin and cut into 7-μm-thick sections, which were then stained with hematoxylin and eosin (H&S) and examined by light microscopy. Scleral thickness was measured in sections passing through the area of electrode-array implantation.

Data analyses

As mentioned previously, a 2D map of reflectance changes was obtained by subtracting raw fundus images taken before from those taken after stimulation. To minimize the effect of blood vessel responses, we analyzed an area of 100 × 100 pixels around the position of the stimulating electrode (Fig. 2a). Positions were identified using raw fundus images. We superimposed the fundus image onto the 2D map of reflectance change and plotted electrode positions on the map.

To evaluate the change in area of reflectance, a GSV of 20 was set as the cutoff to reduce the effect of baseline fluctuations in the 2D map. This value was approximately 4 standard deviations (SD) of the GSV without stimulation. To study the relationship between reflectance change and current amplitude, we summed the GSVs of all pixels in the selected area. This value was named the integrated GSV and used as an indicator of the amplitude of reflectance change. These analyses were performed with Matlab (The MathWorks, Natick, MA, USA) and OriginPro (version 8.5; OriginLab, Northampton, MA, USA). To determine the centroid of reflectance changes, a 2D map of the reflectance changes was converted to intensity images, the GSV of which represented the absolute value of the reflectance change (Fig. 2b). Intensity images were then converted to binary images (Fig. 2c). The threshold level for binarization was adjusted to 30 % of maximum GSV. Using the binary image, the centroid of the white-pixels region was calculated using the Image Processing Toolbox for Matlab. Next, we calculated the ellipse that had the same normalized second central moments as the white-pixels region of the binary images. Cross sections of intensity images were computed along the major and minor axes of the ellipse on intensity images (Fig. 2d). To evaluate the spatial extent of reflectance changes, cross sections were fitted to a Gaussian peak function (Fig. 2e, f), and the full width at half maximum (FWHM) was computed using OriginPro. In some cases, the signal of reflectance change was low, and Gaussian fitting was not possible. In such cases, evaluation of major and minor axes of the ellipse was not done. The Pearson product moment correlation was used to examine the correlation between threshold and other factors. A probability value of <0.05 was considered significant. All statistical analyses were performed using JMP version 9.0 software (SAS Institute, Cary, NC, USA).

Results

Evaluation of porous surface treatment

Scanning electron microscopy confirmed that our surface treatment resulted in a highly pitted surface (Fig. 1a).

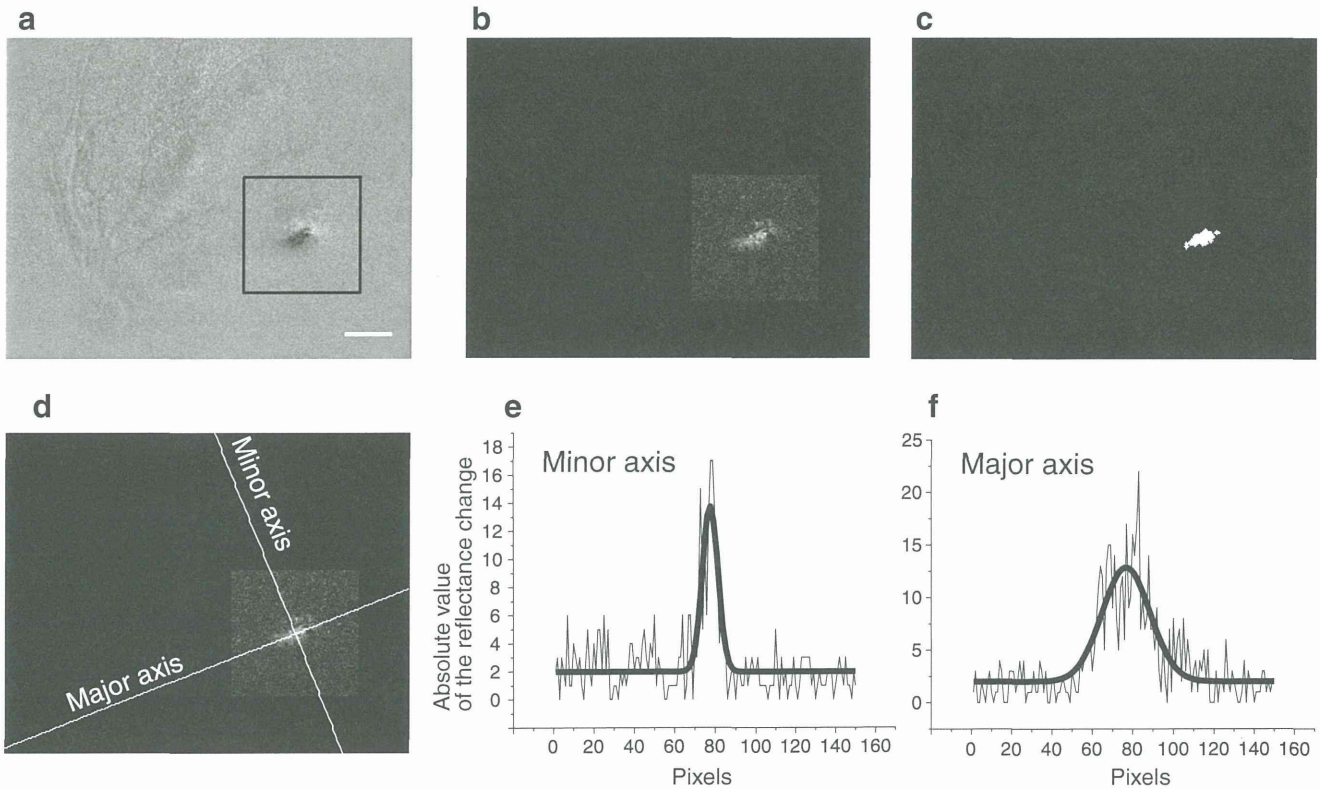

Fig. 2 Calculation of amplitude and spatial extent of reflectance change. **a** Two-dimensional map of reflectance changes 2.0 s after onset of electrical stimulation. To minimize the effect of blood vessel responses, we analyzed areas of 100 × 100 pixels around the electrode array position (*bold line*). *Scale bar* 1 mm. **b** Changes in reflectance in which the absolute value of reflectance change beyond the cutoff value is shown. This image was calculated from (**a**). **c** Intensity image was converted to a binary image. **d** Major and minor axes of the ellipse calculated from (**c**). **e**, **f** Cross sections of grayscale values on the map of absolute value of reflectance changes (**e**, cross section on the major axis; **f**, cross section on the minor axis). The *bold lines* are approximate curves fitted to a Gaussian peak function

Images showed that the pits (size range 1–10 μm) were uniformly distributed along the surface of the platinum bar. In an in vitro impedance test, we observed a three- to tenfold decrease in electrode impedance after the etching process (Fig. 1d). Charge injection capacity of the porous electrode was 1.12 μC/phase in PBS, which was eight times larger than that of the nonporous electrode. These observations demonstrated that the pitted surface increased the electrode surface area.

Time course of reflectance changes in response to electrical stimulation

Examination of the 2D map of reflectance changes after electrical stimulation showed changes in the retinal area where the tip of the electrode adhered to the choroid (Fig. 3a). In a representative case, reflectance change peaked at 2.0–2.5 s after stimulus onset, was sustained for 3.0 s, and then decreased (Fig. 3b). Reflectance changes were observed around blood vessels at about 5.0 s after stimulation onset and about 3.0 s after general reflectance change onset (Fig. 3a).

Electrophysiologic recordings from the optic chiasm following electrical stimulation

The amplitude of electrically evoked potentials recorded in the optic chiasm increased with an increase in stimulus current (Fig. 4a, b). The amplitude of the electrically evoked potential was determined by the first negative peak (latency approximately 3 ms) and the second positive peak (latency approximately 4 ms) (Fig. 4a). The relationship between the amplitude of the electrically evoked potential and the integrated GSV of reflectance changes was assessed in cat no. 5 (electrode Ch 2). Linear regression analysis showed a value of $R^2 = 0.99$, suggesting that reflectance changed linearly with the amplitude of the electrically evoked potential at the optic chiasm (Fig. 4c).

Relationship between reflectance changes and current intensities

The area of reflectance changes increased with currents exceeding the threshold value (Fig. 5a; cat no. 5, electrode Ch1). The integrated GSV of reflectance changes increased

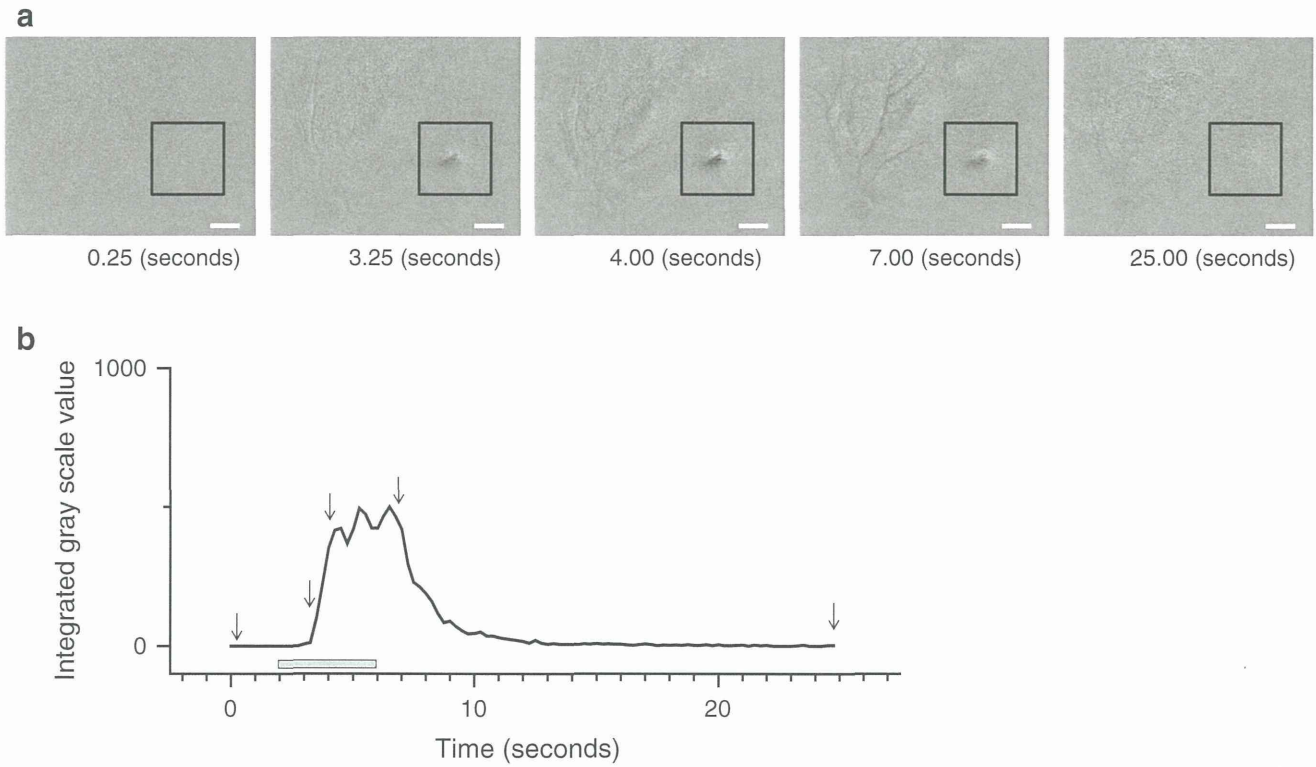

Fig. 3 Time course of reflectance changes after electrical stimulation of the retina. **a** Two-dimensional map of reflectance change at 0.25, 3.25, 4.00, 7.00, and 25.00 s into the trial. Electrical stimulation was applied from between 2.00 and 6.00 s into the trial. Data obtained from cat no. 1, tested with a current of 0.7 mA. The *black square* indicates the area of analysis. *Scale bar* 1 mm. **b** Time course of intensity of integrated gray-scale values of reflectance changes. The *arrows* indicate times when data shown in **a** were obtained. The *gray bar* indicates stimulation period

with an increase in stimulating current (Fig. 5b, c). The threshold current varied among electrodes (410 ± 440 μA; mean ± SD; Fig. 5c) and were defined as the minimum current that evoked a reflectance change of at least 200 integrated GSV.

Area of reflectance changes after electrical stimulation

The average area of reflectance change after a stimulating current of a 1.5 × threshold was 0.42 ± 0.23 mm along the minor axis and 1.46 ± 0.86 mm along the major axis (Table 1). When two different retinal loci were stimulated by passing currents through two different electrodes of the array, distribution of localized signals changed (Fig. 6a–c; cat no. 1). The average distance between the two geometrical centers of retinal reflectance changes was 1.69 ± 0.38 mm when the distance between the two electrodes was 1.5 mm (Table 2).

Relationship between scleral thickness and threshold

The thickness of the sclera on the choroidal side was measured in histologic sections taken through the scleral pocket (Fig. 7a). The threshold current increased with an increase in scleral thickness ($P = 0.0002$; $R^2 = 0.9215$; Fig. 7b).

Relationship between lump height created by the electrode and threshold current

The height of the lump created by the electrode was measured in OCT images (Fig. 7c). Our analysis showed that the threshold current decreased with an increase in lump height created by the electrode array ($P = 0.0111$; $R^2 = 0.6259$; Fig. 7d).

Relationship between impedance and threshold current

The time course of the impedance between the stimulating electrode and the return electrode in vivo showed that the impedance was stable throughout the stimulating trials for up to 17 h. To evaluate the relationship between impedance and threshold current, impedances were measured 15–17 h after onset of the stimulating trial; threshold current decreased with an increase in impedance ($P = 0.0147$; $R^2 = 0.2554$; Fig. 8).

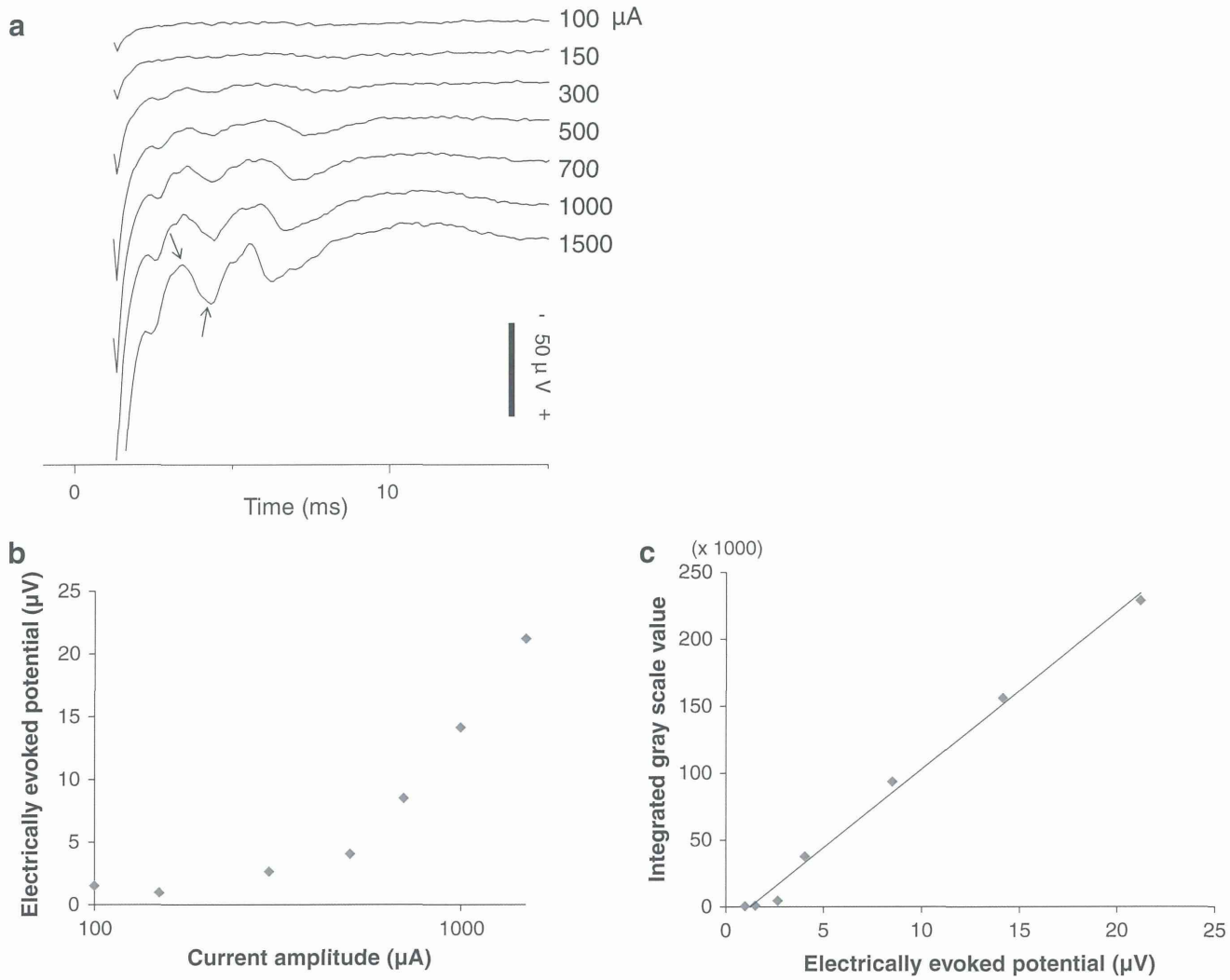

Fig. 4 Potentials evoked by electrical stimulation with the etched electrode in the suprachoroidal–transretinal stimulation (STS) array and recorded at the optic chiasm. **a** Typical electrically evoked potentials recorded at the optic chiasm in response to retinal stimulation. The *left arrow* indicates the first negative peak and the *right arrow* the second positive peak. Data were obtained from cat no. 5 and with electrode Ch2 stimulation. **b** Relationship between the amplitude of electrically evoked potentials and current amplitude. **c** Relationship between integrated gray-scale values of reflectance changes and electrically evoked potentials. The equation for the regression line on the graph is $y = 11{,}728 \text{ x } -14{,}411$ ($R^2 = 0.99$)

Discussion

Previously, we examined the effect of electrical stimulation by a single platinum electrode on the retina using the retinal intrinsic signal in cats and found that electrical currents effectively stimulated local areas of the retina [18]. In the study reported here, we examined the effect of an array of electrochemically treated bulk electrodes (Fig. 1) on eliciting the retinal intrinsic signal. The electrode array was implanted in a scleral pocket, and the procedures were similar to those used in clinical trials [6, 11]. The time course of reflectance changes was relatively slow and similar to that reported previously [18, 19], indicating that reflectance changes do not directly reflect retinal neuronal activity but may be related to vasodynamic processes secondary to excitation of retinal neurons [19] (Fig. 3). The amplitude of the electrically evoked potential at the optic chiasm was significantly correlated with the integrated GSV of reflectance changes, suggesting that the integrated GSV reflected retinal neuronal activity (Fig. 4). The threshold current for reflectance changes varied among eyes, indicating that differences in electrode placement, e.g., distance from the retina and degree of electrical contact to the sclera, might affect the strength of the electrical current that passes to the retina (Fig. 5).

We also stimulated two retinal sites 1.5-mm apart, which resulted in two different retinal areas that responded to stimuli. The distance between centroids of reflectance

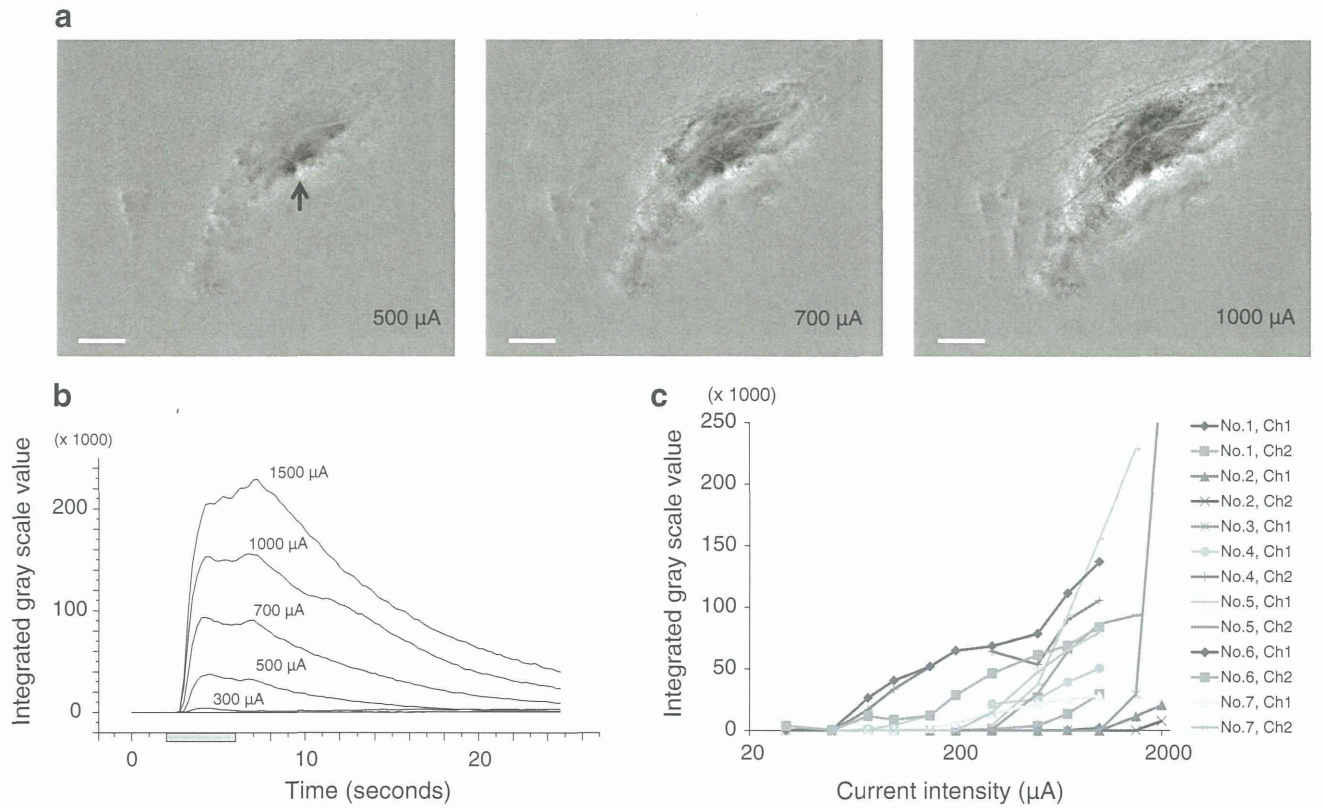

Fig. 5 Relationship between reflectance changes and stimulus currents. **a** Two-dimensional map of reflectance changes 2.00 s after the onset of electrical stimulation with current intensities of 500, 700, and 1,000 μA. The *black arrow* indicates the position of the stimulating electrode. *Scale bar* 1 mm. **b** Intensity time course of integrated gray-scale values (GSV) of reflectance changes. **c** Relationship between integrated GSV of reflectance changes and stimulus current intensities

Table 1 Spatial distributions of reflectance changes

Cat number	Electrode number	Current (μA)[a]	FWHM (mm)	
			Short axis	Long axis
1	Ch1	700	0.29	0.93
1	Ch2	300	0.47	1.20
2	Ch1	1500	0.37	1.51
3	Ch1	1500	0.45	1.61
4	Ch1	100	0.60	3.45
4	Ch2	75	0.16	0.89
5	Ch1	500	0.93	1.34
5	Ch2	500	0.14	0.53
6	Ch1	75	0.31	2.29
7	Ch1	150	0.44	0.80

FWHM full width at half maximum

[a] This current represents a stimulating current of 1.5 × threshold

Table 2 Two-point discrimination

Cat number	Distance between centroids (mm)
1	2.09
4	1.34
5	1.64

changes elicited by the two stimulating electrodes averaged 1.69 mm and was comparable with the distance between the two electrodes. This indicated that two different stimulating sites with a distance of at least 1.5 mm can evoke discriminated responses in the retina using the porous electrode. According to the Gullstrand theoretical exact eye, the length from the nodal point to the retina is approximately 17 mm. Therefore, the distance of 1.5 mm in the human retina corresponds to visual angles of approximately 5.0°, which is equivalent to a visual acuity of 2.5 logMAR units.

In the best result of this study, the FWHM was 0.14 mm along the minor axis and 0.53 mm along the major axis, which correspond to visual angles of approximately 0.5° and 1.8°, respectively. This was comparable with the diameter of the stimulating electrode (0.5 mm). Downsizing the electrode diameter may improve the spatial resolution under optimal conditions.

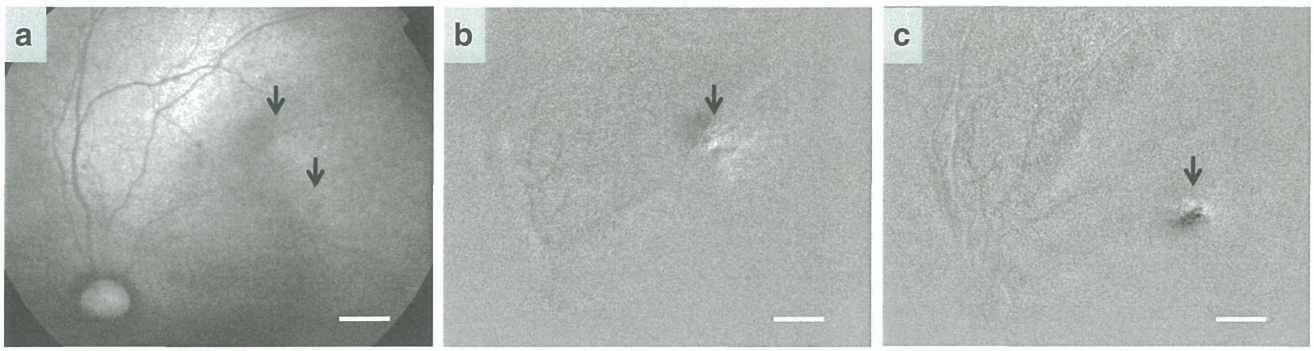

Fig. 6 Reflectance changes in response to electrical stimulation at different retinal loci. **a** Fundus photograph of cat retina. The *left arrow* indicates the position of electrode Ch1 electrode and the *right arrow* the position of the Ch2 electrode. *Scale bar* 1 mm. **b**, **c** Two-dimensional map of reflectance changes 2.0 s after the onset of electrical stimulation (**b** Ch2, 300 μA; **c** Ch1, 700 μA)

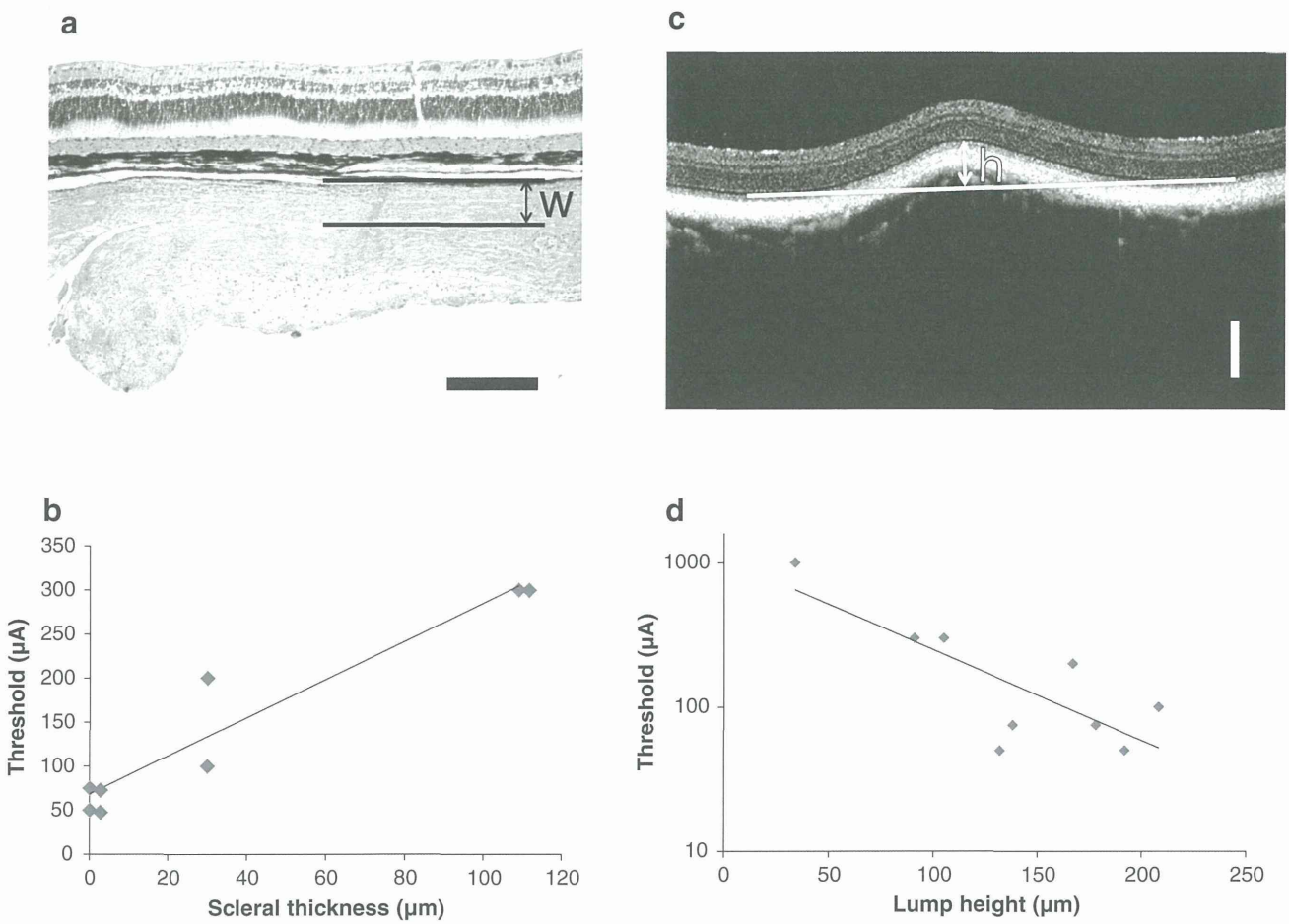

Fig. 7 **a**, **b** Relationship between threshold current and scleral thickness on histology or **c**, **d** lump height on optical coherence tomography (OCT). **a** Histology of retina and sclera where the electrode array was implanted: *w* scleral thickness between scleral pocket and choroid. **b** Relationship between scleral thickness and threshold current. The equation for the regression line is $y = 2.1657x + 68.493$ ($R^2 = 0.92$). **c** OCT image of the retina at electrode position. The height of the lump (*h*), created by the implanted electrode, was obtained from the inner- and outer-segment (IS/OS) line and defined as peak height from baseline. The baseline was a horizontal line (*white line* in **c**), obtained from the tangent of the IS/OS line. *Scale bar* 200 μm. **d** Relationship between lump height and threshold current. The equation for the regression line is $y = 1059.6e^{-0.014x}$ ($R^2 = 0.6259$)

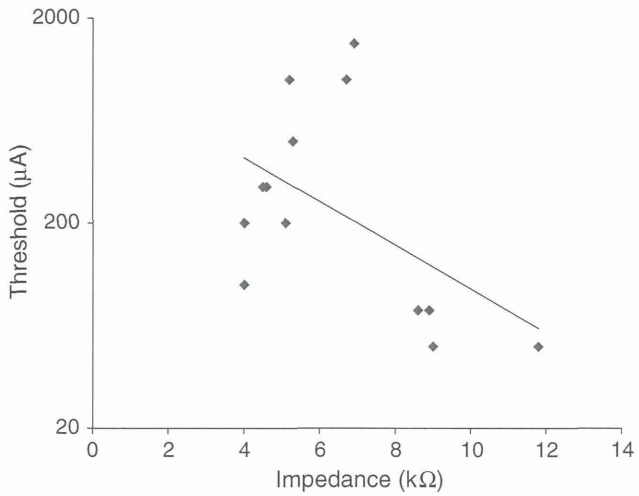

Fig. 8 Relationship between electrode impedance and threshold current. Impedance data were obtained from all cats. The equation for the regression line is $y = 1110.8e^{-0.245x}$ ($R^2 = 0.2554$)

Retinal Implant has created a subretinal prosthesis, which is being tested in clinical trials. Zrenner et al. [2] reported a visual acuity as high as 1.43 logMAR units with this prosthesis. The Argus II retinal prosthesis, from Second Sight Medical Products, is an epiretinal prosthesis and is also being evaluated in a clinical trial. Humayun et al. [5] reported that the best recorded visual acuity with this prosthesis was 1.8 logMAR units. Although it is difficult to compare findings among different clinical trials and in vivo studies, our results suggest that under optimal conditions, e.g., sufficient scleral thickness, STS would allow patients to achieve levels of resolution comparable with those obtained using epiretinal or subretinal prostheses. Furthermore, the electrodes were used to inject 1.12-μC/phase current pulses without exceeding the water window in PBS. This corresponds to 2.2 mA over a 0.5-ms pulse duration. The threshold for retinal response to the STS with the porous electrode was lower than the injection limit. Therefore, the porous electrode can be used effectively to stimulate an STS retinal prosthesis. The threshold current was lower when the thickness of the scleral tissue between the electrode and retina was thinner, indicating that the retina is more effectively stimulated when electrodes are situated closer to the retina (Fig. 7). However, it should be noted that mechanical damage to the retina could be observed when scleral thickness was <80 μm in rabbit experiments (data not shown). Therefore, a balance between scleral tunnel depth and current safety should be obtained. The scleral pocket was surgically created with a crescent knife. However, it is difficult to create a constant scleral pocket depth in every surgical operation. Therefore, residual scleral thicknesses on the electrode surface varied from 0 to 0.1 mm.

Electrode pressure against the choroid and retina was not the same for all experiments. Pressure was affected by scleral pocket depth, width and scleral thickness. For example, pressure was weak when the scleral pocket was wide. Threshold current was lower when the lump created by the underlying electrode was high or electrode impedance was high, which would indicate that a better contact between electrode and sclera may increase electrode impedance. The observation that better contact between electrode and sclera might increase impedance is consistent with reported data [20, 21]. These findings should be useful in creating the optimal scleral pocket.

An advantage of the porous electrode is its high durability. The charge injection capacity of a porous electrode was reportedly kept stable for 1 month of chronic implantation in rabbits [22]. In the study reported here, impedance was also stable throughout the stimulation trials for up to 17 h. These results suggest that porous electrodes have adequate durability for long-term implantation. To demonstrate the superiority of porous electrodes, it may be advisable to compare the difference in results between nonporous and porous electrodes in an in vivo experiment. However, the threshold or localization of response to STS using these electrodes varied with scleral pocket thickness and contact conditions. Therefore, we evaluated the spatial distribution and threshold of neural responses evoked by porous electrodes only. For further comparison of porous and nonporous electrodes, we intend to fabricate a special electrode array.

In conclusion, electrochemically treated porous platinum electrodes are effective in stimulating localized areas of the retina when implanted in a scleral pocket. The threshold current to stimulate the retina was influenced by the thickness of the residual sclera and the firmness of the contact between electrodes and adjacent sclera.

Acknowledgments This study was supported by the Strategic Research Program for Brain Sciences and by a Grant-in-Aid for Scientific Research (A22249058) from the Japanese Ministry of Education, Culture, Sports, Science and Technology, and by a Health Sciences Research Grant (H24-Medical Device004) from the Japanese Ministry of Health, Labor and Welfare.

Conflicts of interest H. Kanda, Grant (NIDEK); T. Mihashi, None; T. Miyoshi, None; Y. Hirohara, Employee (Topcon); T. Morimoto, None; Y. Terasawa, Employee (NIDEK); T. Fujikado, Grant (NIDEK).

References

1. Zrenner E, Bartz-Schmidt KU, Benav H, Besch D, Bruckmann A, Gabel VP, et al. Subretinal electronic chips allow blind patients to read letters and combine them to words. Proc Biol Sci. 2011;278:1489–97.
2. Stingl K, Bartz-Schmidt KU, Besch D, Braun A, Bruckmann A, Gekeler F, et al. Artificial vision with wirelessly powered